Renewable Energy 52 (2013) 273–282

Contents lists available at SciVerse ScienceDirect

Renewable Energy

journal homepage: www.elsevier.com/locate/renene

Optimizing the arrangement and the selection of turbines for wind farms subject to varying wind conditions

Souma Chowdhury [a], Jie Zhang [a], Achille Messac [b,*], Luciano Castillo [c]

[a] Department of Mechanical, Aerospace, and Nuclear Engineering, Rensselaer Polytechnic Institute, Troy, NY 12180, USA
[b] Department of Mechanical and Aerospace Engineering, Syracuse University, Syracuse, NY 13244, USA
[c] Department of Mechanical Engineering, Texas Tech University, Lubbock, TX 79409, USA

ARTICLE INFO

Article history:
Received 1 March 2012
Accepted 22 October 2012
Available online

Keywords:
Cost of energy (COE)
Mixed-discrete optimization
Particle swarm
Turbine selection
Wind distribution
Wind farm layout optimization

ABSTRACT

The development of large scale wind farms that can compete with conventional energy resources presents significant challenges to today's wind energy industry. A powerful solution to these daunting challenges can be offered by a synergistic consideration of the key design elements (turbine selection and placement) and the variations in the natural resource. This paper significantly advances the Unrestricted Wind Farm Layout Optimization (UWFLO) method, enabling it to simultaneously optimize the placement and the selection of turbines for commercial-scale wind farms that are subject to varying wind conditions. The advanced UWFLO method avoids the following limiting traditional assumptions: (i) array/grid-wise layout pattern, (ii) fixed wind condition, or unimodal and univariate distribution of wind conditions, and (iii) the specification of a fixed and uniform type of turbine to be installed in the farm. Novel modifications are made to the formulation of the inter-turbine wake interactions, which allow turbines with differing features and power characteristics to be considered in the UWFLO method. The annual energy production is estimated using the joint distribution of wind speed and direction. A recently developed Kernel Density Estimation-based model that can adequately represent multimodal wind data is employed to characterize the wind distribution. A response surface-based wind farm cost model is also developed and implemented to evaluate and favorably constrain the Cost of Energy of the designed farm. The selection of commercially available turbines introduces discrete variables into the optimization problem; this challenging problem is solved using an advanced mixed-discrete Particle Swarm Optimization algorithm. The effectiveness of this wind farm optimization methodology is illustrated by applying it to design a 25-turbine wind farm in N. Dakota. A remarkable improvement of 6.4% in the farm capacity factor is accomplished when the farm layout and the turbine selection are simultaneously optimized.

1. Introduction

1.1. Wind farm planning – overview

In recent years, growing climate change concerns and unstable fossil fuel prices have increased the focus on sustainable energy resources, such as wind and solar energy. However, the global contribution of wind energy was only 2.5% of the worldwide electricity consumption at the end of 2010 [1]. For wind energy to play a more prominent role in the future energy market, the pressing issues of wind farm under-performance should be particularly addressed. Such advancement can be realized in part through better engineering planning of wind farms.

The engineering planning of a wind farm generally includes (but is not limited to) critical decision-making, regarding

i. the layout of the turbines in the wind farm,
ii. the number of wind turbines to be installed, and
iii. the types of wind turbines to be installed.

Two primary objectives of *optimal wind farm planning* are to minimize the Cost of Energy (COE) expressed in $/kWh, and/or to maximize the net energy production. The energy produced by a farm over a time period is a function of the above-listed design elements and of the variations in the natural resource (primarily the variation of wind speed and direction). Hence, the distribution of wind speed and direction over the concerned time period must be appropriately considered during the planning of a wind farm. A general overview of wind farm optimization is provided in the next section.

* Corresponding author. Tel.: +1 315 443 2341.
E-mail address: messac@syr.edu (A. Messac).

0960-1481/$ – see front matter © 2012 Elsevier Ltd. All rights reserved.
http://dx.doi.org/10.1016/j.renene.2012.10.017

1.2. Wind farm optimization

1.2.1. Literature survey

The total power extracted by a wind farm is in general significantly less than the simple product of "the power extracted by a stand-alone turbine" and "the number of identical turbines (N)" in the farm [2]. This deficiency can be attributed to the loss in the availability of energy due to wake effects – the shading effect of a wind turbine on other turbines downstream from it [3]. Energy deficit due to mutual shading effects is generally determined using wake models that quantify the growth of the wake and the velocity deficit in the wake as functions of the distance downstream from a turbine. Several popular analytical wake models [4–8] and computational wake-flow analysis [9–12] exist in the literature.

The loss of energy due to wake effects can be minimized by careful planning of the placement/arrangement of turbines in a farm, more popularly know as *farm layout* planning. A majority of the methods developed to design wind farm layouts can be classified into the following two class of approaches (see Fig. 1): (i) models that assume an array like (row–column) farm layout [2,13], and (ii) models that divide the wind farm into a discrete grid in order to search for the optimum grid locations of turbines [3,14–17]. Some of the recent methods have made additional important contributions to farm layout decision-making. For example, Gonzalez et al. [16] considers the road layout, the load bearing capacity of the soil, and the presence of other forbidden zones within the farm site in the context of farm layout planning. Chen and MacDonald [17] consider the role of local landowners in the planning of farm layouts.

However, a majority of the existing approaches do not provide the much needed synergistic consideration of (i) the arrangement and (iii) the selection of turbines, as shown by Chowdhury et al. [18]. The energy production capacity of turbines as part of an array strongly depends on the type(s) of turbines installed in the farm – turbines both react to the incoming wind flow and modify the wind flow pattern inside the farm. At the same time, turbines that are more likely to be in the wakes of others throughout the year may face an apparently lower wind class (in their lifetime) than that estimated for a stand-alone turbine at the site. This phenomenon incites an exploration of *the benefits of using multiple types of turbines installed in a particular arrangement in a wind farm*, which is rare in the literature .

In addition, the existing wind farm layout optimization methods make limiting assumptions regarding the resource variations when estimating the energy production over a time period. The nature of wind resource variation (or the lack of it) assumed in the literature can be classified into the following categories:

1. Unidirectional wind with constant speed;
2. Unidirectional wind (or a couple of prevalent wind directions) with a distribution of speed
3. Small number of wind direction sectors each with a speed distribution (like in a windrose diagram)
4. Constant speed wind with equal frequency from all directions

It is evident from this classification that a majority of the wind farm layout optimization methods do not account for the actual *joint distribution* of wind speed and direction. Significant inaccuracies can be introduced into the estimation of the energy production, when such assumptions are made regarding the wind resource variation.

The Unrestricted Wind Farm Layout Optimization (UWFLO) methodology, introduced by Chowdhury et al. [18], avoids the limiting assumptions presented by other methods regarding the layout pattern and partly regarding the selection of turbines. In the UWFLO framework, the turbine location coordinates are treated as continuous variables, which allows all feasible arrangements of the turbines to be considered. This unrestricted layout modeling approach is similar to the approach presented by Kusiak and Zheng [19]. In addition, the original UWFLO method allowed turbines with differing rotor-diameters in order to favorably modify the flow pattern within the farm and increase the net energy production. The original UWFLO framework however assumed a unidirectional and fixed-speed incoming wind, and also did not account for turbines with differing hub-heights and power characteristics. Appropriate consideration of the variation of wind speed and direction and a provision to use multiple types of commercially available turbines are necessary to extend the applicability of the UWFLO methodology to commercial-scale wind farm design.

1.2.2. Objectives of this research

The overall objective of this paper is to significantly advance the original UWFLO methodology by:

i. Estimating and using the joint distribution of the wind speed and direction at the concerned site to determine the annual energy production of the farm;
ii. Modifying the power generation model to allow multiple types of commercial-scale turbines (in the farm), i.e. turbines with differing rotor-diameters, hub-heights, and performance characteristics;
iii. Evaluating the cost of the wind farm using an accurate *Response Surface-based Wind Farm Cost* model (RS-WFC) [20]; and
iv. Implementing a newly developed mixed-discrete Particle Swarm Optimization (PSO) algorithm [21] to solve the wind farm design problem.

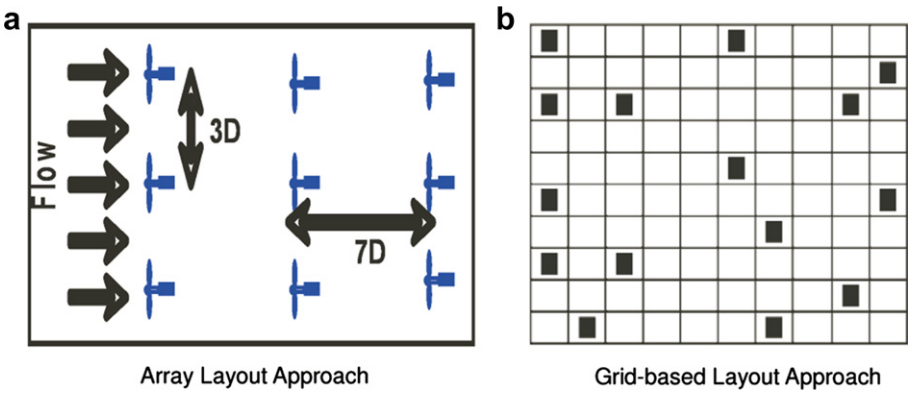

Fig. 1. Existing approaches in wind farm layout optimization (D – turbine rotor-diameter).

To the best of the authors' knowledge, such a comprehensive *optimal wind farm design* strategy is unique in the literature.

The advancements to the UWFLO method is presented in the next section. The application of the advanced UWFLO method and the corresponding results and discussion are presented in Section 3. Section 4 presents the concluding remarks of this research.

2. Advancing the Unrestricted Wind Farm Layout Optimization (UWFLO) method

2.1. Overview of the original UWFLO framework

In the UWFLO power generation model, the growth of the wake behind a turbine is determined using the wake growth model proposed by Frandsen et al. [8]. The corresponding energy deficit behind a turbine is determined using the velocity deficit model presented by Katic et al. [5]. In a wind farm, the velocity of the wind approaching a turbine can be affected by the wake of multiple turbines upstream from it [22]. This wake merging scenario is modeled in the UWFLO method using the wake superposition model developed by Katic et al. [5]. The possibility of a turbine to be 'partially' in the wake of another turbine located upwind is also considered in the UWFLO power generation model. The UWFLO wind farm power generation model has been successfully validated by Chowdhury et al. [18] against published experimental data [23].

Particle Swarm Optimization [24] is applied to optimize the farm layout with the objective of maximizing the total energy production. The farm dimensions and the minimum distance required between any two turbines are treated as system constraints during optimization. In commercial wind farm planning, there are other site-specific factors that might further restrict the arrangement of turbines, such as (i) the topography and the terrain, (ii) the grid connection, (iii) the load bearing capacity of the soil, and (iv) the planned/existing road layout in the farm [16]. The consideration of these site-specific factors are however not within the scope of this paper.

In the following subsections, we briefly discuss how this paper advances the key components of the original UWFLO method. These advanced features provide helpful flexibility to the UWFLO method, and extends its applicability to designing full scale commercial wind farms.

2.2. Estimating the wind farm power generation

Chowdhury et al. [18] modeled the incoming wind as a rotor averaged uniform wind speed, which was estimated from the incoming wind profile reported by Cal et al. [23]. In the case of atmospheric boundary layer, a similarity study can be performed to describe the vertical profiles of turbulence statistics when fully developed conditions are reached [25]. Assuming neutral conditions (negligible thermal effects) in the surface layer, which is applicable for heights less than 100 m, the mean velocity can be represented by the log-profile [25]. For a known measured wind speed U_m at a height z_m, the log-profile can be expressed as

$$\frac{U}{U_m} = \frac{\ln\frac{z}{z_0}}{\ln\frac{z_m}{z_0}} \tag{1}$$

where U represents the wind speed at a height z. The average roughness length in the farm region, represented by z_0 in Eq. (1), depends on the local terrain and type of vegetation. A uniform incoming flow that is equivalent to "*the logarithmic velocity profile (in Eq. (1)) integrated and averaged over the rotor area*" is used in this model.

The wind turbines are assigned fixed X–Y coordinates, from which transformed coordinates can be determined for any given wind direction; the transformed positive X-axis (denoted by x) is always aligned along the wind direction. An inequality was used in the original UWFLO power generation model [18] to determine whether a turbine is in the influence of another turbine; this formulation assumed the two turbines to be identical. In order to allow turbines with differing features, the following new inequality is formulated: Turbine-j is in the influence of the wake created by Turbine-i, if and only if

$$\Delta x_{ij} < 0 \quad \text{and} \quad \sqrt{\left(\Delta y_{ij}\right)^2 + \left(\Delta H_{ij}\right)^2} - \frac{D_j}{2} < \frac{D_{\text{wake},ij}}{2}, \quad \text{where}$$
$$\Delta x_{ij} = x_i - x_j, \quad \Delta y_{ij} = y_i - y_j, \quad \Delta H_{ij} = H_i - H_j$$
$$\forall i, j = 1, 2, \ldots, N; \quad i \neq j \tag{2}$$

In Eq. (2), D_j and H_j are respectively the rotor-diameter and the hub-height of Turbine-j, and H_i is the hub-height of turbine-i. The parameter $D_{\text{wake},ij}$ represents the diameter of the wake produced by Turbine-i and immediately approaching Turbine-j; the growth of the wake diameter with distance downstream from the turbine is estimated using the wake growth model developed by Katic et al. [5]. The parameters x_i and x_j respectively represent the coordinates of turbine-i and turbine-j measured "along" the streamwise direction. The parameters y_i and y_j respectively represent the coordinates of turbine-i and turbine-j measured "perpendicular to" the streamwise direction. The parameter N represents the number of turbines in the farm.

For the given wind direction, the turbines are ranked in the increasing order of their streamwise location. The approaching wind speed for each turbine is then determined in the order of their rank. The wake velocity deficits behind each turbine are determined as functions of the downstream distance, using the 1D wake model proposed by Frandsen et al. [8]. The wake velocity immediately behind the turbine is estimated from the induction factor. A variable induction factor, dependent on the turbine power characteristics and the incoming wind velocity, is used [18]. Considering the possibility of the influence of multiple upstream turbines, a standard wake superposition principle [5] is used to determine the effective speed (U_j) of the wind approaching turbine-j. The possibility of partial wake-rotor overlap [18] is also considered.

The power generated by turbine-j is determined using the turbine power curve, which gives the power generated by the turbine (P_j) as a function of the approaching wind velocity (U_j). However, information regarding the "*power vs. wind speed*" variation is not readily available for every major commercial turbines; generally, the rated power, the rated speed, and the cut-in and cut-out speeds are specified by the turbine manufacturer (in their online brochures). Therefore, a *generalized power curve* (P_n) is developed using the power response data for a popular turbine type: GE 1.5 MW xle [26]. To this end, a 5th degree polynomial is fitted to the power response data, as shown in Fig. 2. As seen from this figure, the power generated (P) by the turbine is normalized using the rated power (P_r) of the turbine, and the incoming wind speed (U) is normalized using the cut-in speed (U_{in}) and the rated speed (U_r) of the turbine.

The *generalized power curve* is assumed to hold for all currently available turbines. This *generalized power curve* is scaled back to represent the approximate power response of a particular commercial turbine, using its rated power (P_r), cut-in speed (U_{in}),

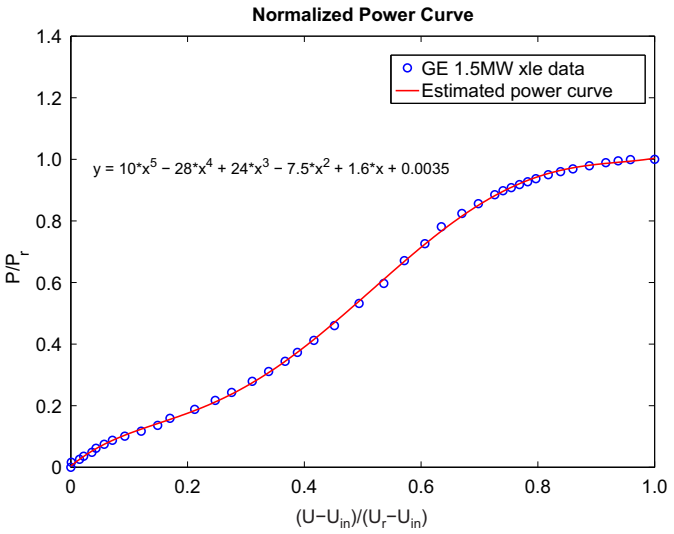

Fig. 2. Power curve of GE 1.5 MW xle turbine.

cut-out speed (U_{out}), and rated speed (U_r) specifications, as given by:

$$\frac{P}{P_r} = \begin{cases} P_n\left(\dfrac{U-U_{in}}{U_r-U_{in}}\right), & \text{if } U_{in} < U < U_r \\ 1, & \text{if } U_r < U < U_{out} \\ 0, & \text{if } U_{out} < U \text{ or } U < U_{in} \end{cases} \quad (3)$$

where P_n represents the polynomial fit for the *generalized power curve*. This generalized power curve method has been used for ready implementation purposes, when considering various types of commercial turbines. However, if the power curve data/expression is available for a particular wind turbine, it can be directly used within the wind farm power generation model.

Therefore, the power generated by any turbine-j is estimated using Eq. (3) and the specifications of that turbine reported by the manufacturer. Once the power generated by each individual turbine has been estimated (in the order of their rank), the net power generated by the farm, P_{farm}, is given by

$$P_{farm} = \sum_{j=1}^{N} P_j \quad (4)$$

where N is the number of turbines in the farm.

2.3. Considering the impact of wind resource variations on the farm output

The power generated by a wind turbine is strongly dependent on the approaching wind speed. The fraction of the energy lost by the wind while flowing across a turbine (often represented by the *induction factor*) also depends on the approaching wind speed. For a given farm layout, the wind direction is another major factor that regulates the overall flow pattern (wake patterns) inside the wind farm. The prediction of the expected annual energy production (AEP) of a wind farm should therefore adequately account for the correlated variations in wind speed and wind direction. To this end, the following two-step procedure is applied:

i. The annual distribution of the wind speed and direction is represented using a suitable probability density function.
ii. The power generation function is integrated over the entire annual wind distribution to yield the AEP.

These two steps are discussed in the following subsections.

2.3.1. Distribution of wind speed and direction

In the literature, one of the most widely-used models for characterizing the wind speed variation is the 2-parameter Weibull distribution [27–29]. Several other distribution models are also used to represent variation of wind conditions, *e.g.*, Rayleigh and Lognormal distributions [29,30]. The direction of wind, which plays an important role in regulating the power generation of a wind farm, also varies with time. Hence, a multivariate probability distribution of the wind speed and wind direction is particularly useful for wind farm layout modeling. To this end, Vega [31] proposed a Weibull distribution that expressed the shape parameter and the scale parameter as stochastic functions of the wind direction.

A majority of the existing wind distribution models make limiting assumptions regarding the dimensionality (univariate assumption) and the modality (unimodal assumption) of the variation in wind conditions. In this paper, a newly developed Multivariate and Multimodal Wind Distribution (MMWD) model [32,33] is used, which avoids such limiting assumptions. This model is developed using multivariate kernel density estimation (KDE) [34]. KDE is an effective non-parametric method of estimating the probability density function of random variables. Further description of the MMWD model can be found in the paper by Zhang et al. [33].

The site used as the case study later in this paper is located at Baker, in North Dakota. The recorded wind data for this site is obtained from the North Dakota Agricultural Weather Network (NDAWN) [35]. We use the daily averaged data for wind speed and direction, measured at the Baker station between the years 2000 and 2009. Description of Baker weather station is provided in Table 1. It is helpful to note that the wind speed data is recorded at a height of 3 m; the log-profile from Eq. (1) is used to determine the wind speed at the pertinent hub-heights. The variation of wind speed and direction at the Baker station is illustrated by a Windrose diagram in Fig. 3. In this diagram, each of the sixteen sectors represent the respective probability of wind blowing from that direction.

2.3.2. Estimating the annual energy production (AEP)

The AEP of a wind farm in kWh (E_{farm}) at a particular location can be expressed as

$$E_{farm} = (365 \times 24) \int_{0^\circ}^{360^\circ} \int_{0}^{U_{max}} P_{farm}(U,\theta) p(U,\theta) \mathrm{d}U \mathrm{d}\theta \quad (5)$$

where, U_{max} is the maximum possible wind speed at that location, and $P_{farm}(U,\theta)$ represents the power generated by the farm (in kW) for a wind speed U and a wind direction θ. In Eq. (5), $p(U,\theta)$

Table 1
Details of the NDAWN station at Baker, ND [35].

Parameter	Value
Location	Baker, ND
Period of record	01/01/2000 to 12/31/2009
Latitude	48.167°
Longitude	−99.648°
Elevation	512 m
Measurement height	3 m

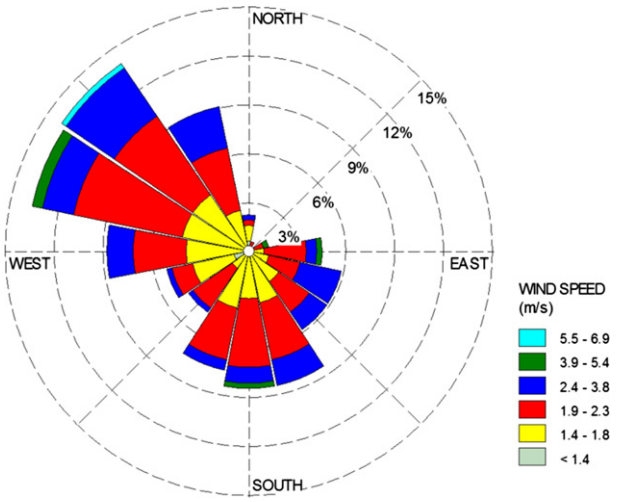

Fig. 3. Windrose diagram for Baker station, ND (Years 2000–2009).

represents the probability of the occurrence of a wind condition defined by speed U and direction θ. The power generated by the entire wind farm is a complex function of the incoming wind properties, the arrangement of turbines, and the turbine features. Hence, a numerical integration approach [19] is suitable for estimating the AEP as given by Eq. (5). To this end, the Monte Carlo integration method is implemented using the Sobol's quasirandom sequence generator. The approximated AEP is readily given by the summation of the estimated power generations ($P_{\text{farm}}(U^i,\theta^i)$) over a set of randomly distributed N_p wind conditions, which is expressed as

$$E_{\text{farm}} = (365\times 24)\sum_{i=1}^{N_p} P_{\text{farm}}\left(U^i,\theta^i\right)p\left(U^i,\theta^i\right)\Delta U\Delta\theta, \quad \text{where}$$
$$\Delta U\Delta\theta = U_{\max}\times 360^\circ/N_p \tag{6}$$

In this equation, the parameters U^i and θ^i respectively represent the speed and the direction of the incoming wind for the ith sample wind condition.

A commonly used measure of wind farm performance is the farm capacity factor. The *capacity factor* of a wind farm can be defined as the ratio of "the actual or expected output of the farm (AEP) over a time period" and "the potential output if the farm was operating at full nameplate capacity throughout that time period". The annual wind farm *capacity factor (CF)* can be expressed in percentage as

$$\text{CF} = \frac{E_{\text{farm}}}{(365\times 24)\sum_{j=1}^{N} P_{rj}}\times 100 \tag{7}$$

where P_{rj} represents the rated power of the jth turbine, and the expression $\sum_{j=1}^{N} P_{rj}$ represents the nameplate capacity of the farm.

2.4. Determining the cost of energy

Numerous models have been developed to evaluate the cost of onshore and offshore wind farms in the last twenty years. Notable examples include: Short-cut model [36], OWECOP-Prob cost model [37], JEDI-wind cost model [38] and the Opti-OWECS cost model [39]. In this paper, we develop and implement a *response surface-based wind farm cost* (RS-WFC) model that is founded on the principles proposed by Zhang et al. [20]. Such a cost model has two major advantages: (i) the cost is represented by a continuous analytical function that can be easily used as a criterion function in optimization irrespective of the search strategy; and (ii) the estimated cost function is helpfully adaptive to the local cost data provided for training the model. In this paper, the estimated annual cost of the farm is represented as a function of *the number of turbines in the farm* and *the turbine rated powers*.

Radial Basis Functions are used to develop the cost response function in this paper. The idea of using Radial Basis Functions (RBF) as approximation functions was introduced by Hardy [40] in 1971. Since then, RBF has been used to approximate multidimensional scattered data for various applications. In creating the cost response function, the annual farm cost is expressed in *dollars per kW installed* (*$/kW*). For a wind farm comprising N turbines, each with rated power P_r, the RS-WFC function, $Cost(P_r,N)$, is expressed as

$$\text{Cost}(P_r,N) = \sum_{i=1}^{n_p}\sigma_i\sqrt{\left(P_r-P_r^i\right)^2+\left(N-N^i\right)^2+c^2} \tag{8}$$

where P_r^i and N^i respectively denote the turbine rated power and the number of turbines in a farm corresponding to the ith training data. The value of the prescribed constant c is specified to be 0.9 in this paper. The generic unknown coefficients, σ_i, are evaluated using the pseudoinverse technique.

In the case of a wind farm comprising different types of turbines, the cost function should be modified. To this end, the total annual cost in dollars can be represented using a more generic expression, as given by

$$\text{Cost}_{\text{farm}} = \sum_{k=1}^{n_t}\text{Cost}\left(P_r^k,N^k\right)\times P_r^k\times N^k \tag{9}$$

where n_t denotes the number of different turbines types used in the wind farm; the parameter N^k represents the number of turbines of type-k in the farm, which have a rated power P_r^k, expressed in kWs. In this case, the total number of turbines (N) in the farm is equal to $\sum_{k=1}^{n_t} N^k$. Subsequently, the COE (in $/kWh) can be estimated as

$$\text{COE} = \frac{\text{Cost}_{\text{farm}}}{E_{\text{farm}}} \tag{10}$$

where E_{farm} is the AEP of the farm in kWh (as given by Eq. (6)).

In this paper, the cost response functions are trained using data provided by the Wind and Hydropower Technologies program (US Department of Energy) [38]. The cost of a commercial wind farm is however a complex function that depends on several other economic and environmental factors/variables as well. The objective of the bivariate cost function developed in this paper is to specifically explore the benefits of (i) optimally selecting the turbine type and (ii) using multiple types of turbines in the farm.

2.5. Formulation of the optimization problem

The objective of the wind farm optimization problem considered in this paper is to maximize the annual energy production for a specified farm-land size and number of turbines. To this end, the advanced UWFLO method simultaneously optimizes the farm layout and the selection of wind turbines. The optimization problem is solved using a Mixed-Discrete Particle Swarm Optimization (MDPSO) algorithm developed by Chowdhury et al. [21,41]. The design variables in the generic optimization problem are the location coordinates of each turbine (continuous variables) and type of the turbine (integer variable). Using the online data

provided by the major turbine manufacturers catering to the US onshore market, an integer code T^k is assigned to each unique turbine-type-k. A turbine-type is defined by a unique combination of rated-power, rotor-diameter, hub-height, and performance characteristics. A list of 66 turbine-types, with rated-powers ranging from 0.6 to 3.6 MW, was prepared and coded from the major turbine manufacturers.

The overall farm optimization problem is defined as

$$\text{Max } f(V) = \frac{E_{\text{farm}}}{(365 \times 24) N P_{r0}}$$

subject to

$$\begin{aligned} & g_1(V) \le 0 \\ & g_2(V) \le 0 \\ & g_3(V) \le 0 \\ & V = \{X_1, X_2, \ldots\ldots, X_N, Y_1, Y_2, \ldots\ldots, Y_N, T_1, T_2, \ldots\ldots, T_N\} \\ & T_i \in \{1, 2, \ldots, T^{\max}\} \end{aligned} \tag{11}$$

where P_{r0} is the rated-power of a reference turbine, which is used to normalize the optimization objective. The parameters T_i and $T^{\max}$ in Eq. (11) respectively represent the type code of the generic ith turbine and the total number of turbine-types considered; and V represents the design variable vector for optimization.

The inequality constraint g_1 represents the minimum clearance required between any two turbines, and is given by

$$g_1(V) = \sum_{i=1}^{N} \sum_{\substack{j=1 \\ j \neq i}}^{N} \max\left((D_i + D_j + \triangle_{\min} - d_{ij}), 0\right), \quad \text{where}$$
$$d_{ij} = \sqrt{\Delta x_{ij}^2 + \Delta y_{ij}^2} \tag{12}$$

In Eq. (12), D_i and D_j represent the rotor-diameters of Turbine-i and Turbine-j, respectively; and $\triangle_{\min}$ is the minimum clearance required between the outer edge of the rotors of the two turbines. In this paper, the value of $\triangle_{\min}$ is set at zero, to allow maximum flexibility in turbine spacing. In practice, a higher value of $\triangle_{\min}$ is necessary to account for factors such as dynamic loading on the turbines.

To ensure the placement of wind turbines within the fixed boundaries of the wind farm-land, the constraint g_2 is specified, which can be expressed as

$$g_2(V) = \frac{1}{2N}\left(\frac{1}{X_{\text{farm}}} \sum_{i=1}^{N} \max\left(-X_i, X_i - X_{\text{farm}}, 0\right) + \frac{1}{Y_{\text{farm}}} \sum_{i=1}^{N} \max\left(-Y_i, Y_i - Y_{\text{farm}}, 0\right)\right)$$

where the parameters X_{farm} and Y_{farm} represent the extent of the rectangular wind farm in the X and Y directions, respectively.

In order to restrict the cost of energy (COE) of a feasible candidate wind farm design to a reference COE, the constraint g_3 is applied. This constraint is defined as

$$g_3(V) = \left(\text{COE} - \text{COE}_{\text{ref}}\right) \Big/ \text{COE}_{\text{ref}} \tag{13}$$

where COE_{ref} is the cost of a farm with an optimized layout and a specified uniform turbine type (reference turbine) having a rated power, P_{r0}. The cost functions are estimated using Eq. (8).

3. Case study: designing a commercial-scale wind farm

3.1. Case study description

In this paper, we explore and compare three different scenarios in the optimal design of a commercial wind farm. In all the three cases, the number of turbines and the farm-land size are assumed to be fixed. The three scenarios are:

Case 1: Optimize the layout of a wind farm that is comprised of a defined turbine-type (reference type).

Case 2: Simultaneously optimize the farm layout and the type of turbine to be installed, considering that a uniform turbine-type is used for the whole farm.

Case 3: Simultaneously optimize the farm layout and the turbine-type of each turbine used in the wind farm, thereby allowing multiple turbine types.

Cases 1, 2 and 3 present $2N$, $2N + 1$, and $3N$ design variables, respectively. The cost constraint, g_3, is applied only in Cases 2 and 3 in order to restrict the COE of feasible farm designs in these cases to the COE of the optimized farm obtained in Case 1 (that uses a fixed uniform turbine type). This cost constraint ensures that the gain in energy production accomplished through the optimal selection of turbine type and/or the use of multiple turbine types is not associated with an increase in the COE of the farm.

The "GE 1.5 MW xle" turbine [26] is chosen as the specified turbine-type in Case 1, and as the reference turbine-type in Cases 2 and 3. The features of this turbine are provided in Table 2. This turbine is reported to be suitable for IEC Wind Class III-b, and has an average velocity specification of 8.0 m/s. For the NDAWN site at Baker, ND, the average wind speed at the reference turbine hub-height (of 80 m) is found to be 8.89 m/s and 8.92 m/s from the estimated wind distribution and the recorded data, respectively. Although, the "GE 1.5 MW xle" turbine is expected to perform well for this site, it may not be the best choice for the given wind conditions at this site. The optimization framework is however not sensitive to this choice, since using a particular specified turbine type is implicit and most likely sub-optimal to the scenario where turbine-types are allowed to vary. For Cases 1 and 2, the PSO algorithm is allowed 200,000 function evaluations. Case 3 presents a more complex mixed-discrete optimization problem, and is therefore allowed 300,000 function evaluations.

All the three case studies are performed for a hypothetical wind farm site at the North Dakota location described in Section 2.3.1. A fixed-size rectangular land is considered for the wind farm comprising 25 turbines. The specified wind farm properties are given in Table 3. The farm is oriented such that the positive X-direction of the layout coordinate system points towards the South. The specified rectangular farm dimensions correspond to a 5×5 array configuration with $7D \times 3D$ inter-turbine spacing.

The prescribed parameters in the mixed-discrete PSO specified for each case is summarized in Table 4. The coefficients α, β_l, β_g, and γ_0 in Table 4, respectively regulate the inertia, the personal behavior, the social behavior, and the diversity preserving behavior of the particles. Further description of these parameters and their

Table 2
Features of the "GE 1.5 MW xle" turbine [26].

Turbine feature	Value
Rated power (P_{r0})	1.5 MW
Rated wind speed (U_{r0})	11.5 m/s
Cut-in wind speed (U_{in0})	3.5 m/s
Cut-out wind speed (U_{out0})	20.0 m/s
Rotor-diameter (D_0)	82.5 m
Hub-height (H_0)	80.0 m

Table 3
Specified wind farm properties.

Farm property	Value
Location	Baker, ND (refer Table 1)
Number of turbines	25
Land size (length × breadth)	$(4 \times 7D_0) \times (4 \times 3D_0)$
Orientation	North to South lengthwise
Average roughness	0.1 m (grassland)
Density of air	1.2 kg/m^3

influence on the dynamics of swarm motion can be found in the papers by Chowdhury et al. [21,41].

3.2. Results and discussion

The optimization converged in Cases 1 and 2. However, Case 3 was only partially converged in the specified number of function evaluations. The convergence histories for the different Cases are shown in Fig. 4. The objective on the *Y*-axis is the normalized annual-average farm power (representative of the net energy production), given by Eq. (11). Further crucial details of the optimized wind farms in the three cases are provided in Table 5. The reference wind farm in Table 5 is comprised of "GE 1.5 MW xle" turbines, arranged in a 5 × 5 array layout with $7D \times 3D$ turbine spacing. The normalized energy production (objective f) and the COE for the reference wind farm is estimated to be 0.597 and \$0.024, respectively.

From Fig. 4, we observe that the maximum improvement in net energy production is accomplished in Case 2. Expectedly, simultaneous optimization of the farm layout and the selection of a uniform turbine-type (Case 2) provided a remarkably higher increase in farm energy production compared to that provided by layout optimization alone. This observation illustrates, *how critically important it is to perform turbine selection in coherence with farm layout design*. However, a lower increase in the energy production in Case 3 compared to Case 2 is counterintuitive since optimal results produced by Case 2 should be suboptimal to, or at least a subset of, the optimal results produced by Case 3. We believe that owing to the significantly higher complexity of the mixed-discrete optimization problem in Case 3 (an additional $N - 1$ discrete variables), only suboptimal results were obtained. Further advancement of the optimization methodology should be able to address this issue.

Table 5 shows that the COE for the optimized farm in Cases 2 and 3 are comparable with Case 1. Progressively higher rated turbines were selected during optimization in Cases 2 and 3, which is one of the factors that helped in the remarkable increase in the farm energy production. The *capacity factor (CF)* of the farm therefore provides a more unbiased measure (than net energy production) of the performance of the optimized farm. As seen from Table 5, the *capacity factors* obtained in Cases 2 and 3 are significantly better than that in Case 1. Furthermore, the *capacity factors* for the optimized farms in all the three cases are observed to be higher by 4.3%–6.4%, when compared to the reference wind farm.

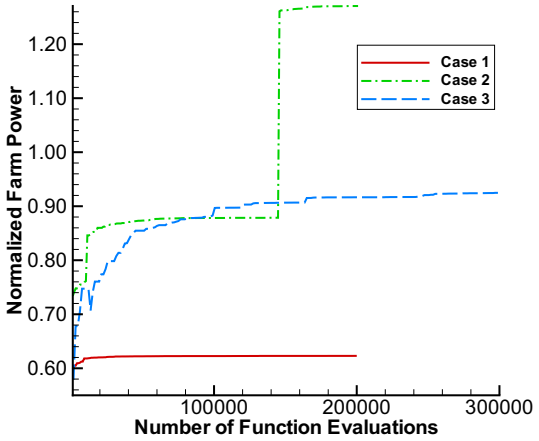

Fig. 4. Convergence histories for the three cases.

The estimated *capacity factors* of the optimized farms and the reference farm are found to be considerably higher than that typical of commercial onshore wind farms (around 20–40%). For example, one of highest recorded annual *capacity factors* is reported to be 57.9% for a 3.68 MW Burradale wind farm at Shetland Islands [42]. In this paper, project-specific power loss factors are not considered, leading to an overestimation of the farm *capacity factor* in the case studies. Project-specific power loss factors include: turbine downtime for O&M, extreme weather conditions, snow accumulation, and curtailments (*e.g.*, noise/environmental curtailment and grid curtailment). The overestimation of the capacity factor can also be partially attributed to a possible underestimation of the wake losses determined by the analytical wake models used in the UWFLO framework.

The turbine-type optimally selected in Case 2 is a 3 MW-112 m wind turbine. In Case 3, the optimized farm is comprised of a combination of eight 1.8 MW-90 m, five 3.0 MW-112 m, four 1.8 MW-100 m, four 2.4 MW-102 m, two 2.0 MW-90 m, one 2.4 MW-95 m, and one 2.5 MW-100 m turbines. The optimized farm layouts for Cases 1 and 2 are shown Figs. 5(a) and (b), where the dashed line represents the farm boundary. The squares that represent the turbine locations are colored according to the annual average power generation of the corresponding turbines. The significantly scattered arrangement of turbines obtained through layout optimization is a noticeable deviation from any array pattern. In Cases 1 and 2, the turbines located on the Eastern edge of the farm produce relatively lower energy over the year. This phenomenon agrees with the Windrose diagram in Fig. 3, which shows that the likelihood of incoming winds from the East is minimal. It is also observed that the differences in the energy production between turbines that generate the maximum and the minimum power annually is only 7.5% and 9.5% for Cases 1 and 2, respectively. This observation indicates an appreciable reduction in wake effects can be achieved through the application of the UWFLO method.

Table 4
User-defined constants in PSO.

Parameter	Case 1	Case 2	Case 3
α	0.5	0.5	0.5
β_g	1.4	1.4	1.4
β_l	1.4	1.4	1.4
γ_0	20	10	10
Population size	$20 \times 2N = 1000$	$20 \times (2N + 1) = 1020$	$20 \times 3N = 1500$
Allowed number of function calls	200,000	200,000	300,000

Table 5
Attributes of the optimized wind farms from the case studies.

Parameter	Case 1	Case 2	Case 3	Reference farm
Normalized AEP (f)	0.623	1.271	0.933	0.597
Farm *capacity factor* (CF)	62.3%	63.5%	63.5%	59.7%
COE (in \$/kWh)	0.023	0.022	0.023	0.024

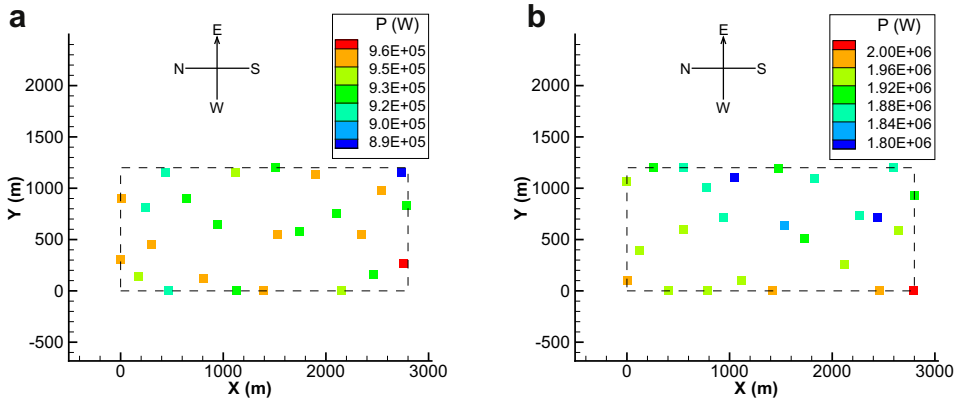

Case 1: Specified turbine-type

Case 2: A single optimally selected turbine-type

Fig. 5. Layouts of the optimized wind farms with identical turbines, showing the individual turbine power generations.

Fig. 6(a), (b), (c) and (d) represent the optimized layout obtained in Case 3, where the turbine locations are colored according to the (i) annual average power generation, (ii) rated power, (iii) rotor-diameter, and (iv) hub-height of the turbines, respectively. It is most interesting to note (from Fig. 6(b)) that the UWFLO has placed the turbines with higher rated-powers on the Eastern edge of the wind farm. These higher rated power turbines are more suitable for lower incoming wind speeds (lower wind classes), as experienced by the Eastern edge of the farm. These higher rated power turbines generally involve larger rotor-diameters as observed in Fig. 6(c). Their location on the Eastern edge of the farm thereby ensures minimal impact of the likely larger wakes created by these turbines.

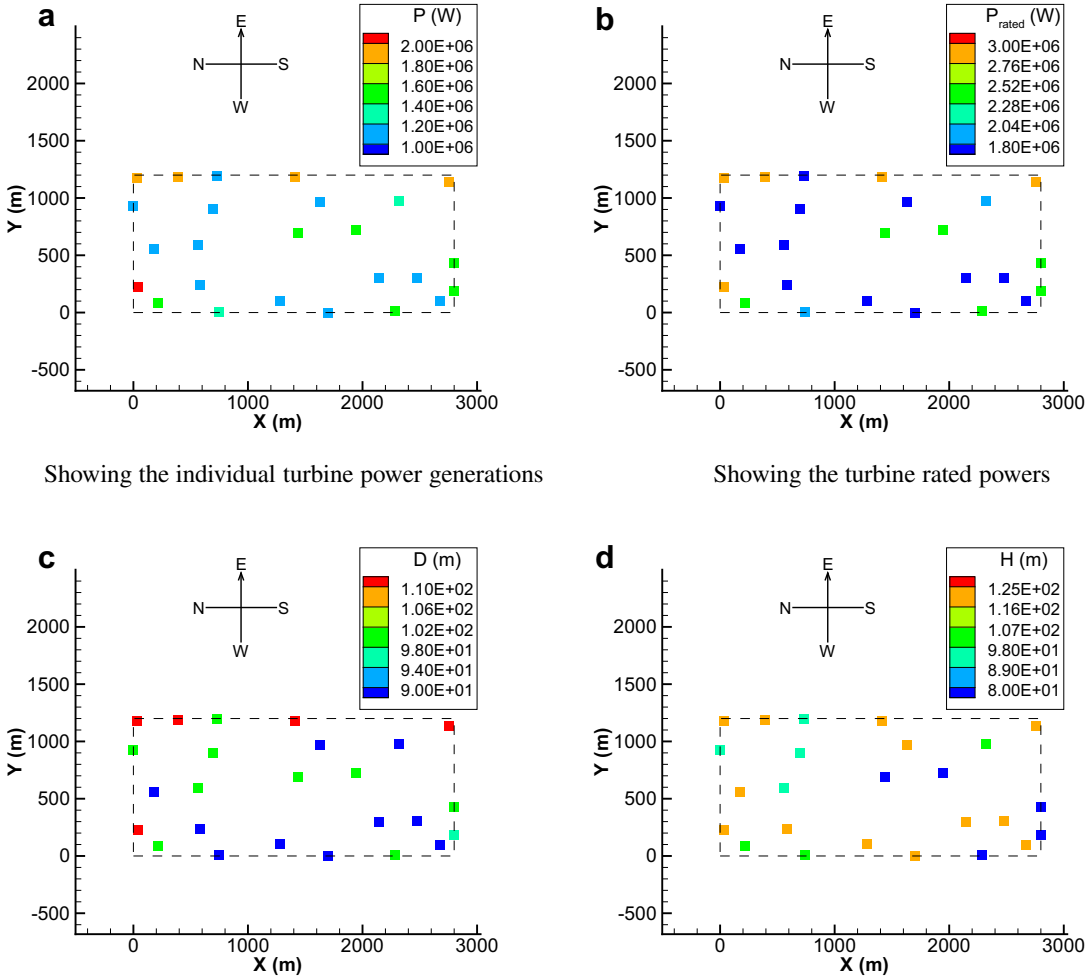

Showing the individual turbine power generations

Showing the turbine rated powers

Showing the turbine rotor-diameters

Showing the turbine hub-heights

Fig. 6. Layout of the optimized wind farm for Case 3 (optimal combination of turbine-types).

4. Conclusion

This paper developed a methodology to design *optimal commercial-scale wind farms*, through significant advancement of the Unrestricted Wind Farm Layout Optimization (UWFLO) methodology. This wind farm design methodology provides optimal decision-making regarding both *what turbines to install* and *where to install them*, which is unique in the wind energy literature. At the same time, the advanced UWFLO method also considers the local long-term variations of wind speed and direction at a site. The wind variations are modeled using an accurate joint distribution of wind speed and direction. The power generation model is modified to account for wind turbines with differing hub-heights and performance characteristics. This modification allows *the use of multiple types of turbines in a wind farm* – a concept that can help increase the capacity factors of future wind farms well beyond what is currently feasible. In order to account for the economic viability of optimizing the selection of turbines, we used a response surface-based wind farm cost model. In this paper, the selection of turbine(s) is primarily based on their overall energy production capacity as members of the array, corresponding to a given wind distribution. In practice, the survivability of turbine components, which depends on its load bearing capacity (given by its IEC ratings), is another important consideration in turbine selection. The incorporation of the survivability of turbine components as an additional design objective is therefore a key topic for future research in optimal turbine selection.

The overall *commercial-scale wind farm design* model presents a complex high-dimensional mixed-discrete optimization problem that is solved using a newly developed mixed-discrete Particle Swarm Optimization algorithm. The new wind farm optimization method is applied to design wind farms comprising 25 turbines on a rectangular farm-land of specified dimensions. Three different farm design scenarios, defined by the turbine selection approach, were explored. Appreciable improvement in the farm performance was observed in each of the three scenarios, when compared to a reference farm with a 5×5 array configuration. Simultaneous optimization of the farm layout and the turbine selection increased the capacity factor by 2% more than that accomplished by layout optimization alone. However, it was found that further improvement in the optimization methodology is necessary to address the challenging scenario where *multiple turbine-types are allowed to be optimally selected*. Overall, it was successfully illustrated that the selection of turbine-type(s) should be performed in coherence with the farm layout planning.

Future work should address the decision-making for other wind farm factors such as the *land area per kW installed* and the *nameplate capacity*, within the context of optimal wind farm design. Together with a more comprehensive cost model, such an advanced *optimal wind farm design* method should provide a strong foundation for future research (and industrial practices) in wind farm planning.

Acknowledgments

Support from the National Science Foundation Awards CMMI-1100948, and CMMI-0946765 is gratefully acknowledged. Any opinions, findings, and conclusions or recommendations expressed in this paper are those of the authors and do not necessarily reflect the views of the NSF.

References

[1] WWEA. World wind energy report 2010, Tech. rep. Bonn, Germany; April 2011.
[2] Sorensen P, Nielsen T. Recalibrating wind turbine wake model parameters – validating the wake model performance for large offshore wind farms. In: European wind energy Conference and Exhibition, EWEA, Athens, Greece; 2006.
[3] Beyer HG, Lange B, Waldl HP. Modelling tools for wind farm upgrading. In: European Union Wind Energy Conference, AIAA, Goborg, Sweden; 1996.
[4] Jensen NO. A note on wind generator interaction. Riso National Laboratory: Roskilde Denmark; 1983.
[5] Katic I, Hojstrup J, Jensen NO. A simple model for cluster efficiency. In: European Wind Energy Conference and Exhibition, EWEA, Rome, Italy; 1986.
[6] Ainslie JF. Calculating the flowfield in the wake of wind turbines. Wind Engineering and Industrial Aerodynamics 1988;27:213–24.
[7] Larsen GC, Hojstrup J, Madsen HA. Wind fields in wakes. In: EUWEC; 1996.
[8] Frandsen S, Barthelmie R, Pryor S, Rathmann O, Larsen S, Hojstrup J, et al. Analytical modeling of wind speed deficit in large offshore wind farms. Wind Energy 2006;9(1–2):39–53.
[9] Jimenez A, Crespo A, Migoya E, Garcia J. Advances in large-eddy simulation of a wind turbine wake. Journal of Physcis: The Science of Making Torque from Wind Conference Series 2007;75(1):012041.
[10] Troldborg N, Sorensen JN, Mikkelsen R. Numerical simulations of wake characteristics of a wind turbine in uniform inflow. Wind Energy 2010;13:86–99.
[11] Calaf M, Parlange MB, Meneveau C. Large eddy simulation study of scalar transport in fully developed wind-turbine array boundary layers. Physics of Fluids 2011;23(12).
[12] Porte-Agel F, Wua Y, Lu H, Conzemius RJ. Large-eddy simulation of atmospheric boundary layer flow through wind turbines and wind farms. Journal of Wind Engineering and Industrial Aerodynamics 2011;99:154–68.
[13] Mikkelsen R, Sorensen JN, Oye S, Troldborg N. Analysis of power enhancement for a row of wind turbines using the actuator line technique. Journal of Physics: Conference Series 2007;75(1).
[14] Grady SA, Hussaini MY, Abdullah MM. Placement of wind turbines using genetic algorithms. Renewable Energy 2005;30(2):259–70.
[15] Sisbot S, Turgut O, Tunc M, Camdali U. Optimal positioning of wind turbines on Gökceada using multi-objective genetic algorithm, lecture notes in computer science. Advances in Swarm Intelligence 2009;13(4):297–306.
[16] Gonzalez JS, Rodriguezb AGG, Morac JC, Santos JR, Payan MB. Optimization of wind farm turbines layout using an evolutive algorithm. Renewable Energy 2010;35(8):1671–81.
[17] Chen L, MacDonald E. A new model for wind farm layout optimization with landowner decisions. In: ASME 2011 International Design Engineering Technical Conferences (IDETC), No. DETC2011-47772. Washington, DC: ASME; 2011.
[18] Chowdhury S, Zhang J, Messac A, Castillo L. Unrestricted wind farm layout optimization (UWFLO): investigating key factors influencing the maximum power generation. Renewable Energy 2012;38(1):16–30.
[19] Kusiak A, Zheng H. Optimization of wind turbine energy and power factor with an evolutionary computation algorithm. Energy 2010;35:1324–32.
[20] Zhang J, Chowdhury S, Messac A, Castillo L. A response surface-based cost model for wind farm design. Energy Policy 2012;42:538–50.
[21] Chowdhury S, Zhang J, Messac A. Avoiding premature convergence in a mixed-discrete particle swarm optimization (MDPSO) algorithm. In: 53rd AIAA/ASME/ASCE/AHS/ASC Structures, Structural Dynamics, and Materials Conference, No. AIAA 2012-1678. Honolulu, Hawaii: AIAA; 2012.
[22] Crespo A, Hernández J, Frandsen S. Survey of modelling methods for wind turbine wakes and wind farms. Wind Energy 1999;2:1–24.
[23] Cal RB, Lebron J, Kang HS, Meneveau C, Castillo L. Experimental study of the horizontally averaged flow structure in a model wind-turbine array boundary layer. Journal of Renewable and Sustainable Energy 2010;2(1).
[24] Kennedy J, Eberhart RC. Particle swarm optimization. In: IEEE International Conference on Neural Networks, no. IV. Piscataway, NJ, USA: IEEE; 1995. p. 1942–8.
[25] Crasto G. Numerical simulations of the atmospheric boundary layer, tech. rep. Cagliari, Italy: Università degli Studi di Cagliari; February 2007.
[26] GE-Energy. 1.5 MW wind turbine, http://www.ge-energy.com/products and services/products/wind turbines/index.jsp [accessed December 2009].
[27] Burton T, David S, Jenkins N, Ervin B. Wind energy handbook. John Wiley & Sons; 2001.
[28] Manwell JF, McGowan JG, Rogers AL. Wind energy explained: theory, design and application. 2nd ed. Chichester, UK: John Wiley & Sons; 2010.
[29] Carta JA, Ramírez P, Velázquez S. A review of wind speed probability distributions used in wind energy analysis case studies in the Canary Islands. Renewable and Sustainable Energy Reviews 2009;13(5):933–55.
[30] Morgan EC, Lackner M, Vogel RM, Baise LG. Probability distributions for offshore wind speeds. Energy Conversion and Management 2011;52(1):15–26.
[31] Vega RE. Wind directionality: a reliability-based approach. Ph.D. thesis, Department of Civil and Environmental Engineering, Texas Tech University: Lubbock, TX; August 2008.
[32] Zhang J, Chowdhury S, Messac A, Castillo L. Multivariate and multimodal wind distribution model based on kernel density estimation. In: ASME 2011 5th International Conference on Energy Sustainability. Washington, DC: ASME; 2011.
[33] Zhang J, Chowdhury S, Messac A, Castillo L. A multivariate and multimodal wind distribution model. Renewable Energy 2013;51:436–47.
[34] Simonoff JS. Smoothing methods in statistics. 2nd ed. Springer; 1996.
[35] NDSU. North Dakota agricultural weather network, http://ndawn.ndsu.nodak.edu/ [accessed December 2010].
[36] Kiranoudis C, Voros N, Maroulis Z. Shortcut design of wind farms. Energy Policy 2001;29:567–78.

[37] Herman S. Probabilistic cost model for analysis of offshore wind energy costs and potential, tech. rep. Energy Research Center; May 1983.
[38] NREL. Jobs and economic development impact (JEDI) model, tech. rep. Golden, Colorado, USA; October 2009.
[39] Cockerill TT. Jobs and economic development impact (JEDI) model. Tech. Rep. JOR3-CT95-0087. Sunderland, USA: Renewable Energy Centre, University of Sunderland; 1997.
[40] Hardy RL. Multiquadric equations of topography and other irregular surfaces. Journal of Geophysical Research 1971;76:1905–15.
[41] Chowdhury S, Tong W, Messac A, Zhang J. A mixed-discrete particle swarm optimization with explicit diversity-preservation. Structural and Multidisciplinary Optimization 2012; http://dx.doi.org/10.1007/s00158-012-0851-z.
[42] REUK, http://www.reuk.co.uk/burradale-wind-farm-shetland-islands.htm, [accessed December 2011].